

See discussions, stats, and author profiles for this publication at: <https://www.researchgate.net/publication/273577989>

# 1D self-assembly of chemisorbed thymine on Cu(110) driven by dispersion forces

ARTICLE *in* THE JOURNAL OF CHEMICAL PHYSICS · MARCH 2015

Impact Factor: 2.95 · DOI: 10.1063/1.4907721 · Source: PubMed

---

READS

15

8 AUTHORS, INCLUDING:



Matthew Stephen Dyer

University of Liverpool

36 PUBLICATIONS 1,041 CITATIONS

[SEE PROFILE](#)



Edward Latter

University of Liverpool

2 PUBLICATIONS 18 CITATIONS

[SEE PROFILE](#)



## 1D self-assembly of chemisorbed thymine on Cu(110) driven by dispersion forces

I. Temprano, G. Thomas, S. Haq, M. S. Dyer, E. G. Latter, G. R. Darling, P. Uvdal, and R. Raval

Citation: *The Journal of Chemical Physics* **142**, 101916 (2015); doi: 10.1063/1.4907721

View online: <http://dx.doi.org/10.1063/1.4907721>

View Table of Contents: <http://scitation.aip.org/content/aip/journal/jcp/142/10?ver=pdfcov>

Published by the AIP Publishing

---

### Articles you may be interested in

[Self-assembly of indole-2-carboxylic acid at graphite and gold surfaces](#)

*J. Chem. Phys.* **142**, 101923 (2015); 10.1063/1.4908143

[Electric field enhancement in a self-assembled 2D array of silver nanospheres](#)

*J. Chem. Phys.* **141**, 214308 (2014); 10.1063/1.4902905

[Self-assembly of enantiopure domains: The case of indigo on Cu\(111\)](#)

*J. Chem. Phys.* **132**, 074705 (2010); 10.1063/1.3314725

[Formation dynamics of hexadecanethiol self-assembled monolayers on \(001\) GaAs observed with photoluminescence and Fourier transform infrared spectroscopies](#)

*J. Appl. Phys.* **106**, 083518 (2009); 10.1063/1.3248370

[Adsorption of  \$\alpha\$ -pyridone on Cu\(110\)](#)

*J. Chem. Phys.* **116**, 8988 (2002); 10.1063/1.1471244

---

A promotional graphic for the new journal APL Photonics. It features a warm orange and yellow background with a sunburst effect. On the left, there's a thumbnail image of the journal cover showing a grayscale microscopy image of a bright spot. A yellow starburst graphic contains the text "OPEN ACCESS". To the right of the image, the text "Launching in 2016!" is written in large, white, sans-serif font, followed by "The future of applied photonics research is here" in a smaller white font. The AIP logo and the journal title "APL Photonics" are at the bottom right.

# 1D self-assembly of chemisorbed thymine on Cu(110) driven by dispersion forces

I. Temprano,<sup>1,a)</sup> G. Thomas,<sup>1</sup> S. Haq,<sup>1</sup> M. S. Dyer,<sup>1</sup> E. G. Latter,<sup>1</sup> G. R. Darling,<sup>1</sup> P. Uvdal,<sup>2,3</sup> and R. Raval<sup>1,b)</sup>

<sup>1</sup>Surface Science Research Centre and the Department of Chemistry, University of Liverpool, Liverpool L69 3BX, United Kingdom

<sup>2</sup>Chemical Physics, Department of Chemistry, Lund University, P.O. Box 124, SE-221 00 Lund, Sweden

<sup>3</sup>MAX-IV Laboratory, Lund University, P.O. Box 118, SE-221 00 Lund, Sweden

(Received 3 November 2014; accepted 26 January 2015; published online 11 February 2015)

Adsorption of thymine on a defined Cu(110) surface was studied using reflection-absorption infrared spectroscopy (RAIRS), temperature programmed desorption (TPD), and scanning tunnelling microscopy (STM). In addition, density functional theory (DFT) calculations were undertaken in order to further understand the energetics of adsorption and self-assembly. The combination of RAIRS, TPD, and DFT results indicates that an upright, three-point-bonded adsorption configuration is adopted by the deprotonated thymine at room temperature. DFT calculations show that the upright configuration adopted by individual molecules arises as a direct result of strong O–Cu and N–Cu bonds between the molecule and the surface. STM data reveal that this upright thymine motif self-assembles into 1D chains, which are surprisingly oriented along the open-packed [001] direction of the metal surface and orthogonal to the alignment of the functional groups that are normally implicated in H-bonding interactions. DFT modelling of this system reveals that the molecular organisation is actually driven by dispersion interactions, which cause a slight tilt of the molecule and provide the major driving force for assembly into dimers and 1D chains. The relative orientations and distances of neighbouring molecules are amenable for π–π stacking, suggesting that this is an important contributor in the self-assembly process. © 2015 AIP Publishing LLC. [<http://dx.doi.org/10.1063/1.4907721>]

## I. INTRODUCTION

The chemical functionalization of surfaces via biologically relevant molecules has attracted great attention in recent years<sup>1–10</sup> due to diverse potential applications in biomimetic surface coatings,<sup>11</sup> organic semiconductors,<sup>12–14</sup> organic photovoltaic devices,<sup>15–17</sup> and biosensors.<sup>18,19</sup> Many of these applications rely on the molecular adlayers being robustly bound and organised into ordered structures at the surface. Given the ubiquity and importance of DNA in natural systems, there is increasing attention on translating DNA components onto surfaces for molecular device applications. The structure and function of DNA are largely determined by the interactions between pairs of four nucleic acids (nucleobases), adenine, cytosine, thymine, and guanine.<sup>20–22</sup> Their individual structures are shown in Figure 1 from which it can be seen that common moieties include amine and carbonyl functional groups. Hydrogen bonding interactions between the bases drive the larger scale conformations of DNA and also lead to the formation of other H-bonded aggregates in 3D systems such as guanine quadruplexes<sup>23</sup> and i-motifs.<sup>24</sup> The propensity for H-bonding, which drives both assembly and base-base molecular recognition, makes nucleobases attractive as motifs for directed molecular self-assembly at surfaces. Similarly,

π–π stacking may play a role in surface ordering as it does in 3D systems<sup>25–27</sup> but this would require the molecules to be orientated to allow for favourable quadrupole interactions. The surface interaction of nucleobases also provides an important stepping stone towards understanding the interaction of single stranded DNA, RNA, and oligonucleotides at surfaces.

The adsorption details and self-assembly of the DNA bases on defined metallic surfaces has recently been reported<sup>28–49</sup> with resultant supramolecular structures dependent on the relative strengths of surface-molecule and inter-molecular interactions. Adsorption on Au(111) surfaces provides an excellent model of nucleobases interacting weakly with the surface. Cytosine<sup>48</sup> and guanine<sup>33</sup> provide prime examples where the weak molecule-surface interaction orients the molecule flat with respect to the surface, leaving key functional groups free to engage in strong, co-operative H-bonding interactions reminiscent of 3D systems; guanine creates H-bonded quadruplexes on Au(111), while cytosine and thymine create zigzag filaments on Au(111), with the latter forming ordered 2D assembly at high coverage. The flat-lying orientation is also observed for guanine, adenine, and cytosine on Cu(111), which also results in 1D and/or 2D self-assembled structures, driven by H-bonding.<sup>29,44,45</sup>

Interaction of DNA bases on Cu(110) provides a contrasting system, where the molecule-surface interaction is stronger and leads to a very different adsorption geometry in which the molecules are held in upright configurations on the surface. Thus, the pyrimidine base molecules, cytosine, thymine,

<sup>a)</sup>Present address: Department of Chemistry, University of Cambridge, Cambridge CB2 1EW, United Kingdom.

<sup>b)</sup>Author to whom correspondence should be addressed. Electronic mail: Raval@liv.ac.uk

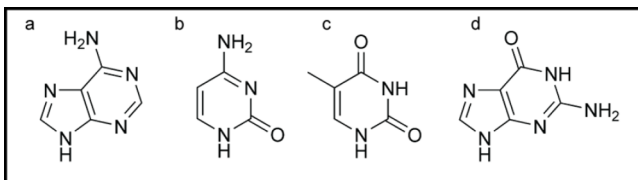


FIG. 1. Molecular structural formulae of DNA nucleobases (a) adenine, (b) cytosine, (c) thymine, and (d) guanine.

and uracil, have been shown to bond in an upright configuration on Cu(110),<sup>35,38,41–43</sup> with adenine also adopting this configuration at higher coverages.<sup>47</sup> The question then arises as to what interactions drive self-assembly in such systems, where the functional groups are not positioned optimally for intermolecular H-bonding interactions as they are for flat-lying species. For the self-organization of upright cytosine on Cu(110), scanning tunnelling microscopy (STM) revealed islands of zigzag chains at low coverage and large ordered domains at monolayer coverage.<sup>28</sup> There is disagreement<sup>28,43</sup> on the exact nature of the adsorbed species but it has been proposed to consist of head-to-head H-bonded cytosine dimer sub-units with orthogonal glide lines present that describe the longer range order.<sup>28</sup>

In this paper, we study the self-assembly of thymine on Cu(110) at room temperature. Temperature programmed desorption (TPD) data indicate that the thymine molecules are deprotonated at room temperature, with our reflection-absorption infrared spectroscopy (RAIRS) and density functional theory (DFT) data confirming that this thymine species adopts an upright orientation aligned along the close-packed [1̄10] rows via three covalent bonds to the surface, in agreement with previous literature.<sup>41</sup> Surprisingly, STM data show 1D assembly in the orthogonal [001] direction. DFT calculations reveal that the observed 1D self-assembly is driven by dispersion interactions between molecules, such as  $\pi$ - $\pi$  stacking, leading to the unexpected assembly direction.

## II. METHODS

### A. Experimental

RAIRS experiments were carried out using an ultra-high vacuum (UHV) chamber interfaced with a Mattson 6020 FTIR spectrometer via ancillary optics and KBr windows. A nitrogen cooled HgCdTe detector allowed the spectral range of 650–4000 cm<sup>-1</sup> to be accessed. The spectrometer was operated with a resolution of 4 cm<sup>-1</sup>, with the addition of 256 scans to collect each spectrum. The spectra were recorded throughout a continuous dosing regime as sample single beam infrared spectra, and ratioed against a reference background single beam representing the clean Cu(110) surface. TPD data were acquired with a VG Micromass mass spectrometer, which enabled the main mass fragments of the molecule at atomic mass unit (AMU) 55 and 82 to be monitored along with H<sub>2</sub> at AMU 2.

STM images were acquired using a Specs STM 150 Aarhus instrument, calibrated by measuring the specific distances of the O(2 × 1) superstructure following the adsorption of oxygen onto the clean Cu(110) surface. All measurements

were taken in constant current mode using a tungsten tip. Bias voltages are measured at the sample ( $V = V_{\text{sample}}$ ). STM images were enhanced using WSXM and Image SXM.<sup>50</sup>

Cu(110) crystals (Surface Preparation Laboratory, NL) were cleaned by cycles of Ar<sup>+</sup> ion bombardment and annealing to ~800 K, until a sharp (1 × 1) LEED pattern characteristic of clean Cu(110) was observed. Thymine (≥99% Sigma-Aldrich) was used as purchased and, following degassing cycles at ~340 K, was sublimed onto the clean Cu(110) surface, held at 300 K, via a specially constructed glass Knudsen cell, separated from the main chamber by a gate valve and differentially pumped by a turbomolecular pump.

### B. Periodic DFT calculations

The periodic DFT calculations in this study were performed using version 5.2 of the plane-wave basis set VASP code.<sup>51,52</sup> The standard ultra-soft pseudopotentials were used with the PW91 version of GGA,<sup>53</sup> requiring a plane-wave cut-off energy of 396 eV. Except where stated, molecules were adsorbed in a 6 × 5 slab supercell containing four Cu layers, with the top two layers allowed to relax. Reciprocal space was sampled with a 5 × 3 × 1 Monkhorst-Pack  $k$ -point set. Dipole corrections were included in the direction perpendicular to the surface. For dispersion corrected calculations, the Grimme method<sup>54</sup> was employed. The component for Cu–Cu interactions was omitted such that the Grimme dispersion corrections included were those between atoms within the molecules and between the surface and molecule atoms only. STM simulations were computed using the Tersoff-Hamann approximation as implemented by Lorente and Persson.<sup>55,56</sup>

The adsorption energies per molecule,  $E_{\text{ads}}$ , were computed from

$$E_{\text{ads}} = (E_{\text{total}} - E_{\text{metal}} - nE_{\text{thymine}} - nE_{\text{H-ads}}) / n, \quad (1)$$

where for  $n$  molecules,  $E_{\text{total}}$  is the energy of the fully relaxed structure,  $E_{\text{metal}}$  is the energy of the clean, relaxed metal slab, and  $E_{\text{thymine}}$  is the energy of an isolated thymine molecule in the gas-phase.  $E_{\text{H-ads}}$  accounts for the hydrogen lost on adsorption and is computed from

$$E_{\text{H-ads}} = E_{\text{H+slab}} - E_{\text{slab}}, \quad (2)$$

where  $E_{\text{H+slab}}$  is the total energy of a hydrogen atom adsorbed on a metal slab of a 6 × 5 supercell of Cu(110), and  $E_{\text{slab}}$  is the energy of the clean 6 × 5 Cu(110) slab, i.e., our adsorption energies are referenced to hydrogen adsorbed on the surface.

### C. Vibrational spectra

Electronic structure calculations of infrared spectra have been performed with the Gaussian09<sup>57</sup> package using a cluster of eleven copper atoms to represent the surface. We used the hybrid density-functional method B3LYP and the 6-311+G(d,p) basis set, which gives converged frequencies with respect to addition of diffuse functions and polarization functions.<sup>58</sup> During the optimization, all copper atoms were frozen at the corresponding bulk separation of 2.55 Å. The anharmonicity of the vibrational modes of the present system were treated with an experimental scaling factor of

0.9843 which normalizes the  $\nu_s(\text{C}-\text{O}) + \delta(\text{NH})$  mode to the experimental value at  $1625 \text{ cm}^{-1}$ . This scaling factor gives a better agreement with experiment than the general scaling factor 0.9679 determined by Andersson and Uvdal<sup>58</sup> for the 6-311+G(d,p) basis set making the mode assignment more transparent.

### III. TAUTOMERISM OF NUCLEIC ACIDS

The four bases of DNA, displayed in Figure 1, can exist in various tautomeric forms. Nucleobase tautomerism is responsible for inducing alterations in the normal base pairing, increasing the risk of spontaneous mutations in DNA and RNA.<sup>59,60</sup> Adenine and cytosine display amino-imino tautomerism, while guanine and thymine can exist in either keto or enol forms. All tautomeric forms of each base exist in equilibrium, but the amino and keto forms are more stable than the neutral chemical form of the nucleobases.

Thymine is known to exist in its neutral di-keto form in the gas phase, in aqueous solution, and in the solid polycrystalline state.<sup>61,62</sup> The anionic form resulting from deprotonation of one of the nitrogen atoms has been observed in metal complexes, alkali salts, and in adsorption on metal surfaces.<sup>31,63</sup> The resultant mono-anionic species exhibits two tautomeric structures, which are distinguished by the position of deprotonation. One tautomer arises from deprotonation at the N(1) position, the other from the N(3) position. The electronic structure of each tautomer can be described in terms of a resonance delocalised bond system, whereby the negative charge is delocalised in the  $\pi$ -orbitals of the heterocyclic ring and the exocyclic oxygen atoms. The resonant structures and delocalised form are shown in Figure 2. The relative stabilities of these species are affected by their environments, such as bonding to a metal atom.

### IV. RESULTS AND DISCUSSION

#### A. Chemical nature of the adsorbed motif

TPD data recorded after the adsorption of a saturated monolayer of thymine on Cu(110) at 86 K (Figure 3) show a number of hydrogen desorption features, suggesting successive dehydrogenations of the molecule as the surface

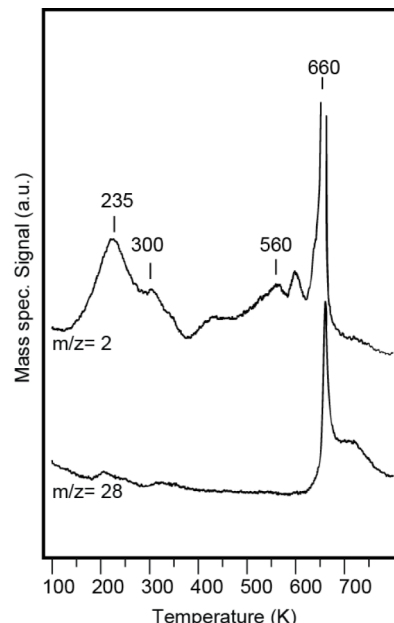


FIG. 3. TPD spectra obtained for a saturated monolayer of thymine adsorbed at 86 K. Masses corresponding to desorption of  $\text{H}_2$  ( $m/z = 2$ ) and  $\text{CO}$  ( $m/z = 28$ ) were monitored.

temperature is increased. Anionic thymine, in which dehydrogenation occurs at the nitrogen positions, has been previously reported in the literature under different conditions.<sup>31,38,41,42,63,64</sup> The first dehydrogenation occurs at  $\sim 235 \text{ K}$ , with further dehydrogenation processes observed above  $400 \text{ K}$  leading to a broad desorption peak from  $400$  to  $600 \text{ K}$ , which is in agreement with the study by McNutt *et al.*<sup>46</sup> Molecular decomposition occurs at  $660 \text{ K}$  as shown by sharp and simultaneous desorption of  $\text{H}_2$  and  $\text{CO}$ . These high temperature phases are not considered in the present work.

Here, we focus on the room temperature phase, which is preceded by the hydrogen desorption peak at  $\sim 235 \text{ K}$ . Dehydrogenation is believed to occur from the N(3) position between the carbonyl groups. Previous angle-resolved UV photoemission spectroscopy (ARUPS),<sup>35</sup> Photoelectron Diffraction (PhD),<sup>41</sup> near-edge X-ray absorption fine structure (NEXAFS),<sup>41,42</sup> and soft X-ray photoelectron spectroscopy (SXPS)<sup>49</sup> studies consistently suggest that the adsorbed thymine species created at room temperature possesses two

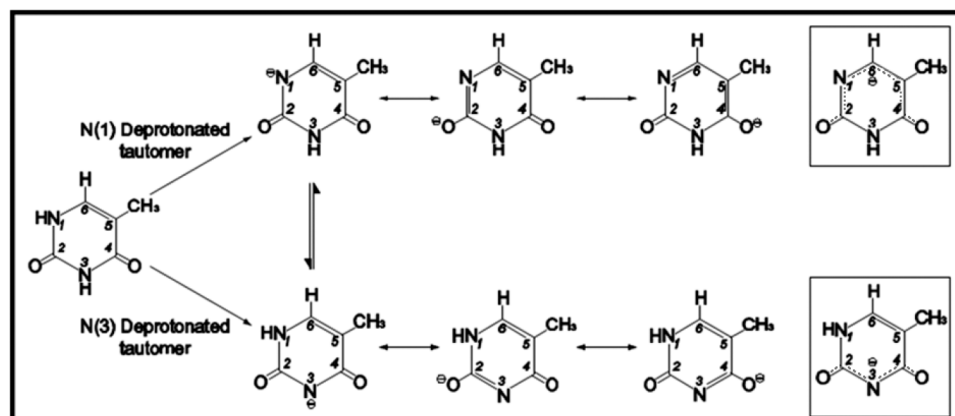


FIG. 2. Molecular structure of thymine, with the atoms numbered according to the standard system adopted for DNA bases. Each tautomer is represented in terms of three extreme resonance structures, with the actual molecule being a resonance hybrid of all three.

essentially equivalent O atoms but two inequivalent N atoms. This has been interpreted in terms of a single dehydrogenation of the N(3) atom located between the two carbonyl groups. Allegretti *et al.*<sup>41</sup> have elucidated a detailed structural model in which the singly dehydrogenated thymine adopts a three-point-contact bonding configuration, where bonding to the surface occurs through both the carbonyl O atoms and the dehydrogenated N(3) atom, with each occupying a near-atop site on the close-packed rows. Additionally, this work shows that the molecular plane is strongly aligned along the close-packed [1̄10] direction and is held near perpendicular to the surface with a small tilt of about 20°.

## B. DFT calculations for an isolated dehydrogenated thymine adsorbed on Cu(110)

In order to understand the adsorption configuration and energetics, DFT calculations were performed for an isolated, singly dehydrogenated thymine adsorbed in two different configurations, aligned along and across the close-packed rows on the surface, Figures 4(a) and 4(b), respectively. In agreement with experimental data, the results show that there is a very strong preference (by 0.51 eV, see Figure 4) for the molecule to adsorb with its molecular plane aligned along the close-packed rows in the [1̄10] direction, Figure 4(a), rather than across the rows in the [001] direction, Figure 4(b). Overall, with inclusion of dispersion interactions, there is a high chemisorption energy of -2.2 eV for the preferred configuration, reflecting the three-point interaction with the underlying surface via strong O–Cu and N(3)–Cu bonds. The O–Cu and N–Cu bonds are all approximately 2.0 Å in length with the O–Cu bond at the C(2) position being consistently 1% longer, reflecting a slightly lower charge on the O due to the

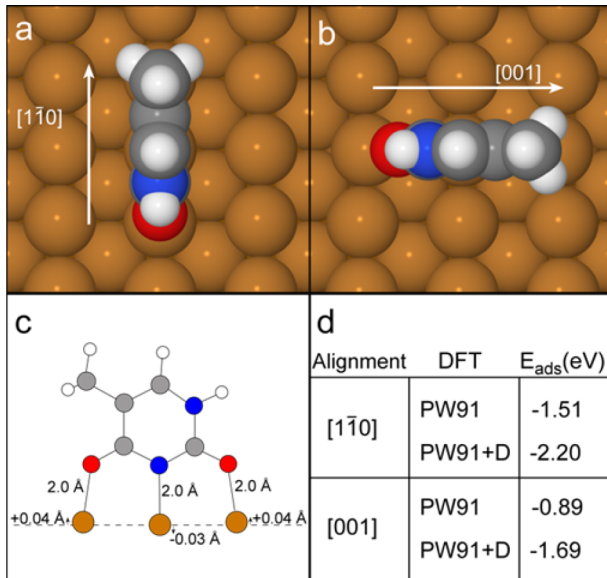


FIG. 4. Thymine deprotonated at the N(3) position adsorbed (a) with the molecular plane aligned along the close-packed [1̄10] direction and (b) adsorbed across the rows, i.e., with the molecular plane in the [001] direction. (c) Schematic view of the favoured adsorption configuration in (a) obtained with PW91+D calculations. (d) Adsorption energies of the two configurations computed with (+D) and without dispersion corrections.

electron withdrawing nature of the N–H group. Using PhD, Allegretti *et al.*<sup>41</sup> also report inequivalent Cu–O bond lengths (1.91 Å and 2.03 Å), which represents a variation of closer to 5%. Their study also concluded that the Cu–N bond length is  $1.96 \pm 0.02$  Å. These small discrepancies between experiment and theory are not formally significant, since adsorbate-substrate bond lengths found from DFT calculations are characteristically longer than those found from experiment.<sup>43</sup> Our results also show that the molecule does not fit perfectly on three adjacent Cu sites; consequently, the Cu atom bonding to the N is depressed by ~0.03 Å, while those under the O atoms are pulled out of the surface by ~0.04 Å, as indicated in Figure 4(c). The Cu–N bond length reported here of 2.0 Å is in good agreement with that for the adsorption of pyridine<sup>65</sup> and 2-methyl-pyridine on Cu(110).<sup>66</sup> Finally, there is no preference for tilting of the plane of this isolated species. In fact, the tilt mode is extremely soft, with negligible energy difference incurred by inducing a tilt on the isolated molecule.

## C. Experimental and calculated RAIRS of thymine on Cu(110) at 300 K

Vibrational spectroscopic data on the system were obtained in order to provide further information on adsorption geometry. Figure 5(b) shows the experimental RAIR spectrum recorded for a saturated monolayer of thymine adsorbed on

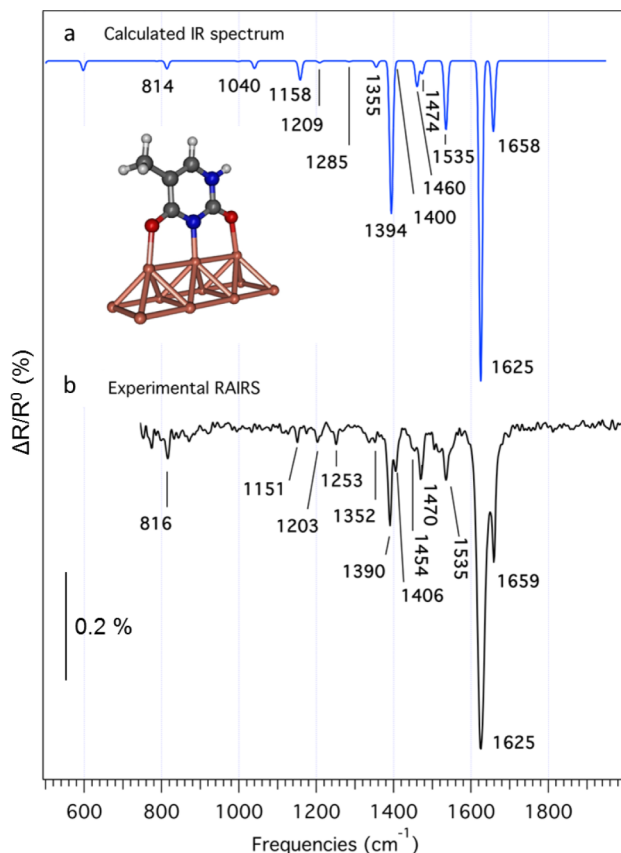


FIG. 5. (a) Spectrum computed for a single anion of thymine on Cu(110) shown in Figures 4(a) and 4(c) using GaussView.<sup>57</sup> (b) Experimental RAIR spectrum obtained for a saturated monolayer of thymine adsorbed on Cu(110) at 300 K.

TABLE I. Vibrational assignments for RAIRS data obtained experimentally for a saturated monolayer and calculations of an isolated anion of thymine adsorbed on Cu(110) at 300 K. (Note: the intensities expected for a RAIRS experiment have been calculated to only include components of the dynamic dipole moments normal to the surface.)

Thymine on Cu(110) experimental ( $\text{cm}^{-1}$ )	Calculated ( $\text{cm}^{-1}$ )	Expected RAIRS intensity of calculated modes	Character	Approx. mode assignment
	578	0	A'	
	597	8	A'	
	638	1	A'	
	746	0	A''	
	762	0	A''	
773	787	0	A'	Ring + $\nu(\text{N}-\text{Cu})$
816	814	7	A'	Ring + $\rho(\text{CH}_3)$
	884	0	A'	
	997	0	A'	
	1040	7	A'	
	1050	0	A'	
1151	1158	18	A'	$\delta(\text{NH}) + \delta(\text{CH})$
1203	1208	2	A'	Ring + $\nu(\text{C}-\text{CH}_3)$
1253	1285	0	A'	
1352	1355	6	A'	Ring + $\delta(\text{CH})$
1390	1394	144	A'	$\nu_{\text{as}}(\text{C}-\text{O}) + \delta(\text{NH}) + \nu_{\text{s}}(\text{CNC})$
1406	1400	1	A'	$\delta_{\text{s}}(\text{CH}_3)$
	1447	0	A''	
1454	1460	24	A'	Ring + $\delta(\text{NH}) + \delta_{\text{as}}(\text{CH}_3)$
1470	1474	12	A'	Ring + $\delta_{\text{as}}(\text{CH}_3)$
1535	1535	65	A'	$\nu_{\text{as}}(\text{C}-\text{O}) + \delta(\text{NH}) + \delta_{\text{as}}(\text{CH}_3)$
1625	1625	302	A'	$\nu_{\text{s}}(\text{C}-\text{O}) + \delta(\text{NH})$
1659	1658	69	A'	ring(C-C)
2928	2985	14	A'	$\nu_{\text{s}}(\text{CH}_3)$
	3038	0	A''	
3029	3057	20	A'	$\nu_{\text{as}}(\text{CH}_3)$
	3150	4	A'	
3458	3568	72	A'	$\nu(\text{NH})$

Cu(110) at 300 K. The experimentally determined spectrum is compared with the calculated one, Figure 5(a), which has been computed based on the single molecule configuration shown in Figure 4(a) using Gaussian09.<sup>57</sup> All the calculated modes are listed in Table I with predicted intensities, character (A' are in-plane and A'' are out-of-plane modes), and approximate mode assignments (based on inspection using GaussView3). To account for the metal-surface selection rule, the intensities only include components of the dynamic dipole moments normal to the surface, i.e., in the C<sub>s</sub> plane of the molecule and perpendicular to the Cu–Cu–Cu bond direction. By comparing Figures 5(a) and 5(b), it can be seen that there is a high level of agreement between experiment and theory for the frequency and absorption intensity of each mode, providing further support for a three-point-contact model with the thymine adsorbed with its ring standing approximately upright from the surface. We note that, for this system, the RAIR spectrum is not able to discern small tilts of the molecular plane with respect to the surface normal. A tilt could, in principle, induce some intensity to out-of-plane modes but they will most likely remain very weak for small tilt angles. Table I shows the peak positions and assigned vibrational modes for both the experimental and calculated spectra. Most of the calculated infrared modes are a combination of vibrations and only the highly contributing

motions for each vibrational frequency have been identified in order to simplify the discussion.

The experimental RAIR spectrum has a noticeable absence of carbonyl stretching vibrations in the region between 1670  $\text{cm}^{-1}$  and 1800  $\text{cm}^{-1}$ . Peaks in that region are symptomatic of stretching  $\nu_{\text{s}}(\text{CO})$  of strongly ketonic carbonyl groups, and their absence suggests a more enolic character in the adsorbed molecule. Indeed, this is also what is indicated by the DFT calculations. The full monolayer spectrum of thymine adsorbed at 300 K is dominated instead by a peak at 1625  $\text{cm}^{-1}$  which corresponds to a strongly red-shifted  $\nu_{\text{s}}(\text{CO})$  mode coupled with a  $\delta(\text{NH})$  vibration. The presence of strong peaks at 1535  $\text{cm}^{-1}$  and 1390  $\text{cm}^{-1}$  both arise from the  $\nu_{\text{as}}(\text{CO})$  vibrations, with the former coupled with  $\delta(\text{NH}) + \nu_{\text{s}}(\text{C}-\text{N}-\text{C})$  vibrations, and the latter with  $\nu_{\text{as}}(\text{C}-\text{O}) + \delta(\text{NH})$  vibrations. The coupling of  $\nu_{\text{as}}(\text{CO})$  with  $\nu_{\text{s}}(\text{CNC})$  in the mode appearing at 1390  $\text{cm}^{-1}$  is a strong indication that both C–O bonds are coupled to each other through the resonance delocalised bond system, [O–C–N–C–O]<sup>-</sup>.<sup>46</sup> Finally, the presence of a number of intense bands associated with in-plane vibrations of the ring structure, along with the absence of out-of-plane modes, is a further indication of a predominantly vertical orientation of the molecule, in agreement with the proposed three-point-contact model shown in Figures 4(a) and 4(c).

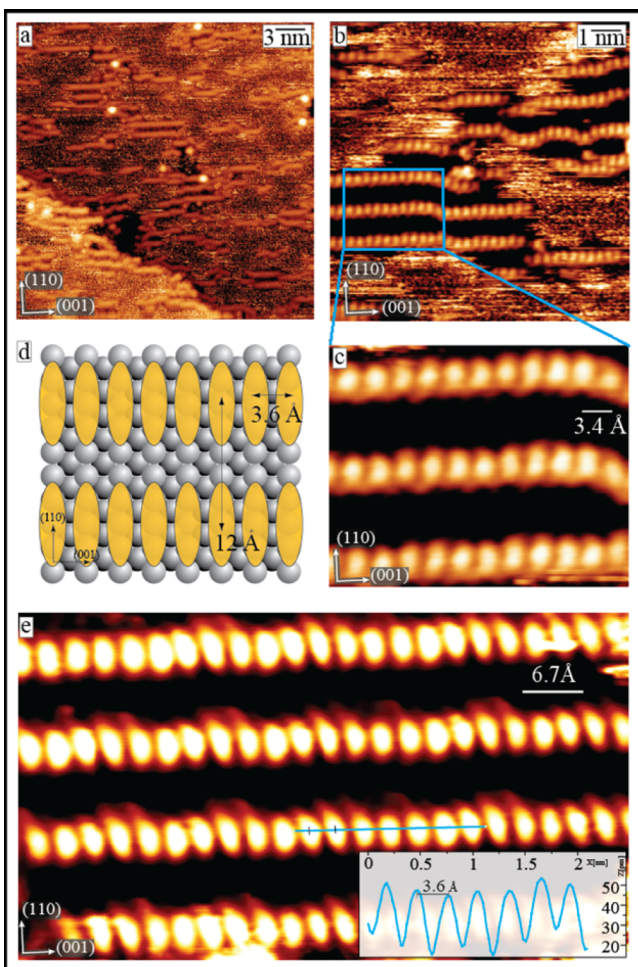


FIG. 6. Constant current STM images of thymine adsorbed on Cu(110) dosed and recorded at room temperature: (a)  $30 \times 30 \text{ nm}^2$  image ( $I_t$ :  $-0.430 \text{ nA}$ ;  $V_t$ :  $-611.3 \text{ mV}$ ) of several 1D thymine chains including a step edge with assembled molecules following the contour. Further detail of the 1D chains is recorded in smaller-area images: (b)  $10 \times 10 \text{ nm}^2$  image ( $I_t$ :  $-0.330 \text{ nA}$ ;  $V_t$ :  $-305.8 \text{ mV}$ ) and (c)  $3.4 \times 2.8 \text{ nm}^2$ . (d) Schematic model of the 1D self-assembled row of thymine, represented by the yellow ovals possessing appropriate molecular dimensions, and showing inter-molecular repeat distances of  $3.6 \text{ \AA}$  and inter-chain distance of  $12 \text{ \AA}$ . (e) High resolution  $6.7 \times 3.8 \text{ nm}^2$  image ( $I_t$ :  $-0.390 \text{ nA}$ ;  $V_t$ :  $-437 \text{ mV}$ ) with line profile analysis showing a  $3.6 \text{ \AA}$  repeat in the [001] direction.

#### D. STM of self-assembled 1D chains of thymine on Cu(110)

Large area STM images, Figures 6(a) and 6(b), obtained after the adsorption of thymine on Cu(110) at 300 K show molecular self-assembly into 1D chains that are preferentially orientated along the open-packed [001] direction of the metal surface. Higher-resolution, small-area STM images, Figures 6(c) and 6(e), show that the self-assembled thymine chains consist of a series of bright, oval-shaped protrusions packed parallel to each other. The approximate size of the individual protrusions ( $2 \text{ \AA} \times 5 \text{ \AA}$ ) is consistent with the molecular dimensions of thymine and we, therefore, assign each protrusion to an individual adsorbed thymine species. Additionally, a highly regular packing arrangement is observed, with every protrusion separated by  $\sim 3.6 \text{ \AA}$ , which coincides with the open-packed distance on the Cu(110) surface. This repeat distance is consistent with a 1D close packing arrangement of thymine

molecules on consecutive Cu rows as depicted in the schematic model in Figure 6(d). Local islands which possess an array of 1D chains show that, typically, large inter-chain distances of more than  $12 \text{ \AA}$  are maintained, suggesting that minimal chain-to-chain interaction occurs.

#### E. DFT calculations of 1D self-assembled chains of thymine on Cu(110)

##### 1. Dimer assembly

Periodic DFT calculations were carried out in order to gain a better understanding of the 1D molecular chain assembly at the surface. To represent the first step in chain growth, a dimer was formed by placing molecules on adjacent close-packed rows. Despite this being a simple assembly, a number of combinations need to be considered. First, the methyl groups can be chosen to be on the same or alternate sides of the molecules and, second, the molecules can be upright or tilted. This gives four possible configurations for the dimer, as shown in Figure 7. DFT calculations reveal that the relative positions of the methyl groups make negligible difference to the total energy of the dimer, suggesting that both conformations are expected to occur in equal measure. Tilting the molecules also only causes a very small decrease in the total energy suggesting that, as for the isolated molecule, the rocking mode is very soft. The net result is that a dimer with methyl groups on opposite ends of the molecules, and with both molecules tilted by  $\sim 20^\circ$  in the same direction is the most favoured configuration, with a binding energy of  $-2.33 \text{ eV/molecule}$ , Figure 7(d). However, there is only a small energy difference between this and the other three configurations, as can be seen in Figure 7. We note that the

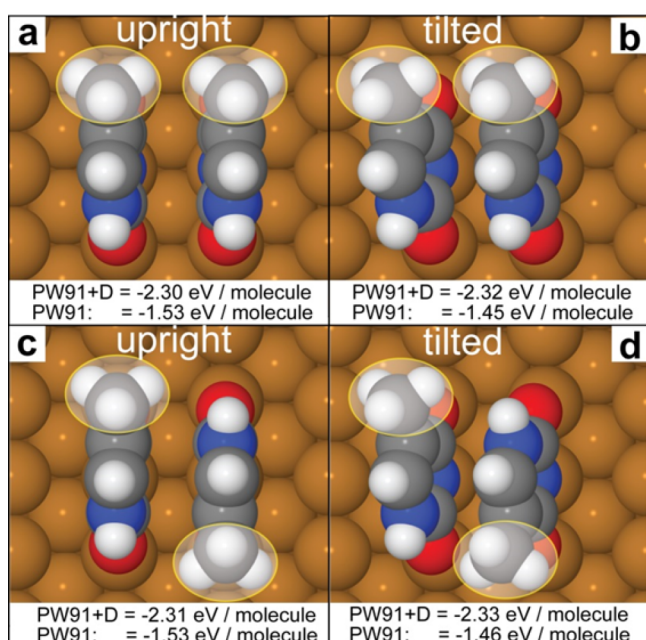


FIG. 7. The four modelled configurations for thymine dimers on Cu(110). Configurations (a) and (b) have the methyl groups on the same end of each molecule, whilst in configurations (c) and (d) they are on opposite ends. Configuration (d), with methyl groups on opposite ends and molecules tilted by  $\sim 20^\circ$  to the surface normal, has the best binding energy of  $-2.33 \text{ eV/molecule}$ .

inter-molecular interaction provides a slightly more favourable binding energy for the dimer by 0.13 eV/molecule compared to the isolated molecule, *but this is only the case when dispersion forces are included*. Without dispersion forces, the dimer is only 0.02 eV more favourable than the single molecule, an energy difference that lies within the error limits of the calculation. The basic bonding to the surface, however, is unchanged in the dimer and the details of the Cu–O and Cu–N bonding are the same as those of the isolated molecule.

## 2. 1D infinite chain assembly

DFT calculations for an infinite self-assembled chain running in the [001] direction show that if dispersion interactions are included, the binding energy becomes more favourable for long chains than for a dimer and reaches a minimum value of  $-2.41$  eV as shown in Table II. There is now also a clear preference for the tilting of the whole row of molecules by  $\sim 20^\circ$ , which also reduces the repulsion between the methyl groups. However, the relative positioning of the methyl groups along the chain does not affect the energetics significantly; there is only a negligible improvement of 10 meV if the methyl groups are positioned alternately along the chain. This small energy difference suggests that the methyl groups will be randomly distributed on either side of the molecular chain.

STM simulations were carried out for the upright and tilted 1D chain assemblies in which the methyls were arranged alternately as shown in Figure 8. The STM simulation for the tilted configuration in Figure 8(c) is clearly comparable to the experimentally determined image in Figure 6(e) with the bright protrusions coinciding with the positions of the molecules. We note that this image is formed primarily from tunnelling from the  $\pi$  states of the molecular ring. This is shown more clearly in the STM simulation for the chain of upright molecules shown in Figure 8(f), where there is one bright feature per molecule, but the features are clearly located *between* molecules corresponding to areas of high  $\pi$  electron density. Overall, the tilted molecular configuration shown in Figures 8(a) and 8(b), closely corresponds to the geometry deduced by the PhD studies of Allegretti *et al.*<sup>41</sup>

TABLE II. Binding energies for infinite 1D chains of thymine molecules computed with dispersion interactions and molecules upright or tilted to the surface normal, and with the methyl groups either all on one side of the molecule (aligned), or on opposite sides for any two neighbouring molecules (alternating).

Configuration		$E_{\text{ads}}$ /eV PW91+D
Methyls aligned	Upright	-2.31
	Tilted	-2.40
Methyls alternating	Upright	-2.35
	Tilted	-2.41

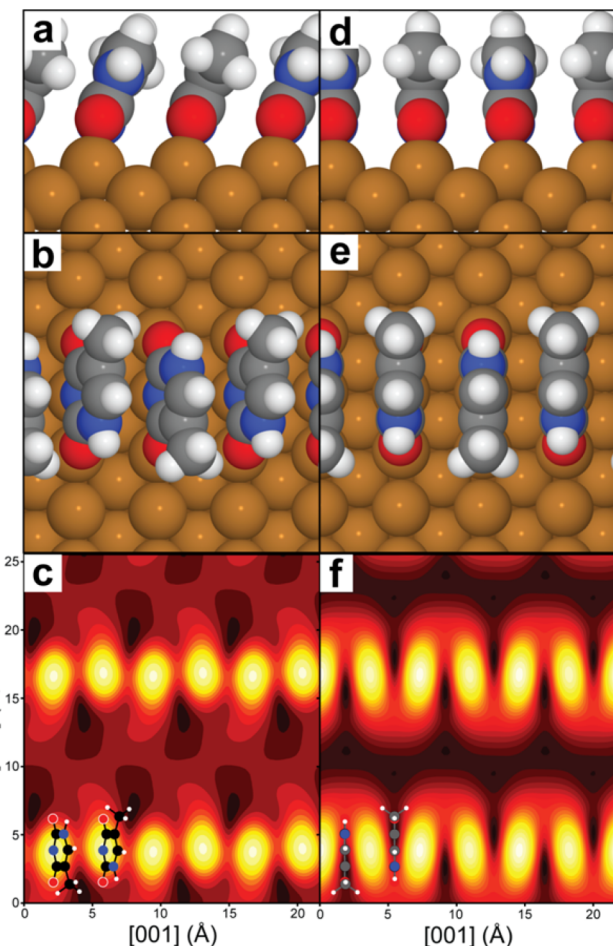


FIG. 8. (a) and (b) The most favoured 1D infinite thymine row structure, with molecules tilted at  $20^\circ$  to the surface normal and methyl chains alternating on either side along the chain. (c) Simulated STM image of most favoured structure showing a single bright protrusion located on each molecule. (d) and (e) The structure of the upright, methyl alternating configuration. (f) STM simulation for upright, methyl alternating configuration showing that the STM is imaging the  $\pi$  electrons lying between the molecules, rather than the top of individual molecules.

## F. DFT calculations: Impact of dispersion interactions and tilt

Our DFT calculations reveal that the adsorption energetics are governed by three factors: copper-thymine binding, the tilt angle of the molecules, and most importantly for self-assembly of rows, the inter-molecular dispersion interactions. The relative strength of these varies for the monomer, dimer, and infinite chain as can be seen in Figure 9.

At all coverages, the binding of the molecules to the surface is predominantly through strong O–Cu and N–Cu bonds, which contribute over 1.4 eV per molecule to the binding energy. This is largely the same for all coverages and the critical bond lengths shown in Figure 4(c) are also unchanged. In the absence of dispersion forces, an upright configuration is favoured for all coverages, representing monomer, dimer, and chain assembly, as can be seen in Figure 9(a). Thus, DFT calculations without dispersion do not reproduce the experimental finding that the molecules are tilted by  $\sim 20^\circ$  at higher coverage and wrongly suggest that the upright configuration would be favoured in the 1D chain assembly by approximately 0.05 eV.

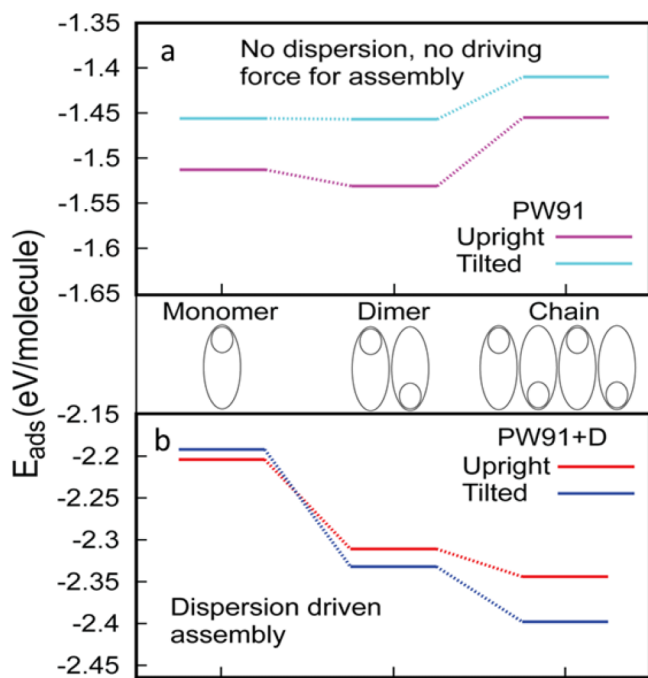


FIG. 9. Binding energy per molecule for increasing coverage from monomer to a complete chain of molecules with methyl groups alternating along the chain. (a) The top panel shows results computed without dispersion corrections, and an upright adsorption geometry is favoured, but 1D chain formation is unfavourable. (b) The bottom panel shows that inclusion of dispersion corrections<sup>53</sup> yields stronger bonding as the coverage increases, with tilting favoured for all but an isolated molecule.

Turning to the driving force for assembly, it can be seen from Figure 9(a) that increasing the coverage from isolated molecules to dimers gives a small, almost negligible, difference in binding energy. Remarkably, the main conclusion that can be drawn from Figure 9(a) is that in the absence of dispersion corrections, the DFT predicts that the molecular chains, tilted or otherwise, will *not* form, as repulsion between the molecules destabilizes the chains relative to the isolated molecules. This result is clearly at odds with the STM images in Figure 6 and additional factors need to be included in the DFT calculations to accurately describe the experimental observations.

Figure 9(b) shows the adsorption energetics when dispersion interactions are included in the calculations and these are in good agreement with the experimental findings. For the single molecule, the adsorption energy becomes more favourable by about 0.7 eV with dispersion interactions, as can be seen in Figure 4(d), and the difference between upright and tilted orientations effectively disappears. When the coverage is increased to form an adsorbed dimer, there is an increase in the net binding per molecule and, for the first time, the observed tilt of ~20° is favoured over the upright configuration. In other words, dispersion forces are responsible for binding the molecules more strongly to the surface, for inducing the tilted orientation, and for favouring the dimer assembly. Further increasing the coverage to complete the molecular chains improves the adsorption energy by another ~70 meV and the tilted orientation becomes more favoured still. It is apparent that, as for the dimers, molecules in the chains are held together by the dispersion forces and they provide about 1 eV of the binding energy per molecule (as can be seen by comparing

Figures 9(a) and 9(b)), providing a significant driving force for the assembly into 1D chains. We also note that for the 1D chains held together by dispersion forces, the separation distance of 3.4–3.6 Å between molecules closely resembles the packing of aromatic molecules in 3D systems governed by π-π stacking,<sup>27,67</sup> suggesting that such interactions may be a primary driver of self-assembly at the Cu(110) surface.

Overall, it can be surmised from the DFT calculations that the interaction of the thymine molecule to the copper surface, via O–Cu and N–Cu covalent bonds, is the driving force for the initial adsorption to occur. However, the self-assembly into ordered 1D chains is driven by the favourable dispersion interactions, such as π-π interactions, which are sufficient to overcome the repulsion between the molecules. This is reminiscent of biological systems, where there is strong chemical bonding within local structures, but large-scale structures are determined by the balance of repulsive forces (here, repulsion between the molecular rings) and attractive forces, which include dispersion interactions.<sup>68</sup>

## V. CONCLUSIONS

This paper has described in detail the 1D self-assembly of thymine anions on a Cu(110) surface at room temperature under UHV conditions. TPD data show a single deprotonation occurring below room temperature. The interaction with the surface occurs between the two carbonyl groups and the deprotonated N(3) atom with three Cu atoms of a single (110) row. Experimentally measured and calculated RAIR spectra confirm a largely upright positioning of the anionic form of thymine with respect to the surface and a three-point-contact for the molecule-surface binding is proposed which is in good agreement with other studies reported in the literature. This mode of surface binding is in agreement with the mode assignments of the vibrational frequencies in the RAIR spectra, particularly the coupling of the  $\nu_{as}(\text{CO})$  and  $\nu_s(\text{CNC})$  which results in a peak at 1390 cm<sup>-1</sup>.

STM images show a series of ordered 1D chains indicative of an energetically favourable self-assembly process. The orientation and chemical nature of the molecule exclude H-bonding as the dominant form of inter-molecular interaction, in contrast to what is often observed for DNA bases self-assembled on surfaces. In order to ascertain the relative importance of surface-molecule and inter-molecular interactions and investigate the driving forces for the self-assembly process, DFT calculations were carried out. The DFT calculations of adsorption of an upright dimer (the first stage in chain assembly) reveal that there is a high surface-molecule binding energy and a slightly tilted orientation of ~20° is favoured. The dimer is only more favoured over the isolated molecules when dispersion interactions are included in the DFT calculations. The preference for a small tilt angle over the upright configuration and the need to include dispersion interactions is even more apparent when the self-assembled, infinite 1D chain is modelled. In particular, DFT calculations without dispersion forces included indicate that an isolated molecule or dimer would be favoured over the experimentally observed 1D chains. Thus, dispersion interactions are central to driving the 1D chain self-assembly of thymine on Cu(110), with the

juxtaposition and separation distance of 3.4–3.6 Å between adjacent molecules closely resembling the packing of aromatic molecules in 3D systems governed by π–π stacking.<sup>27,67</sup>

## ACKNOWLEDGMENTS

We thank the EPSRC (EP/F00981X/1) for supporting part of the experimental programme on assembly at surfaces. Gaussian09 calculations were performed on the Linux cluster at Lunarc, the Center for Scientific and Technical Computing for Research at Lund University. Via our membership of the UK's HPC Materials Chemistry Consortium, which is funded by EPSRC (EP/L000202), this work made use of the facilities of HECToR and ARCHER, the UK's national high-performance computing service, which is funded by the Office of Science and Technology through EPSRC's High End Computing Programme.

- <sup>1</sup>S. M. Barlow, S. Louafi, D. Le Roux, J. Williams, C. Muryn, S. Haq, and R. Raval, *Langmuir* **20**, 7171–7176 (2004).
- <sup>2</sup>S. M. Barlow and R. Raval, *Surf. Sci. Rep.* **50**, 201–341 (2003).
- <sup>3</sup>S. M. Barlow and R. Raval, *Curr. Opin. Colloid Interface Sci.* **13**, 65–73 (2008).
- <sup>4</sup>M. Forster, M. S. Dyer, M. Persson, and R. Raval, *Angew. Chem., Int. Ed.* **49**, 2344–2348 (2010).
- <sup>5</sup>M. Forster, M. S. Dyer, M. Persson, and R. Raval, *J. Am. Chem. Soc.* **133**, 15992–16000 (2011).
- <sup>6</sup>S. Haq, A. Massey, N. Moslemzadeh, A. Robin, S. M. Barlow, and R. Raval, *Langmuir* **23**, 10694–10700 (2007).
- <sup>7</sup>B. Kasemo, *Surf. Sci.* **500**, 656–677 (2002).
- <sup>8</sup>S. J. Sowerby, N. G. Holm, and G. B. Petersen, *Biosystems* **61**, 69–78 (2001).
- <sup>9</sup>G. M. Whitesides and B. Grzybowski, *Science* **295**, 2418–2421 (2002).
- <sup>10</sup>G. M. Whitesides, J. P. Mathias, and C. T. Seto, *Science* **254**, 1312–1319 (1991).
- <sup>11</sup>B. D. Ratner, *J. Mol. Recognit.* **9**, 617–625 (1996).
- <sup>12</sup>C. D. Dimitrakopoulos, S. Purushothaman, J. Kymmissis, A. Callegari, and J. M. Shaw, *Science* **283**, 822–824 (1999).
- <sup>13</sup>J. E. Green, J. Wook Choi, A. Boukai, Y. Bunimovich, E. Johnston-Halperin, E. DeIonno, Y. Luo, B. A. Sheriff *et al.*, *Nature* **445**, 414–417 (2007).
- <sup>14</sup>V. C. Sundar, J. Zaumseil, V. Podzorov, E. Menard, R. L. Willett, T. Someya, M. E. Gershenson, and J. A. Rogers, *Science* **303**, 1644–1646 (2004).
- <sup>15</sup>M. Granstrom, K. Petritsch, A. C. Arias, A. Lux, M. R. Andersson, and R. H. Friend, *Nature* **395**, 257–260 (1998).
- <sup>16</sup>N. S. Sariciftci, L. Smilowitz, A. J. Heeger, and F. Wudl, *Science* **258**, 1474–1476 (1992).
- <sup>17</sup>G. Yu, J. Gao, J. C. Hummelen, F. Wudl, and A. J. Heeger, *Science* **270**, 1789–1791 (1995).
- <sup>18</sup>J. Fritz, M. K. Baller, H. P. Lang, H. Rothuizen, P. Vettiger, E. Meyer, H.-J. Güntherodt, C. Gerber, and J. K. Gimzewski, *Science* **288**, 316–318 (2000).
- <sup>19</sup>S. B. Smith, L. Finzi, and C. Bustamante, *Science* **258**, 1122–1126 (1992).
- <sup>20</sup>R. E. A. Kelly and L. N. Kantorovich, *J. Phys. Chem. B* **110**, 2249–2255 (2006).
- <sup>21</sup>S. J. Sowerby, M. Edelwirth, and W. M. Heckl, *J. Phys. Chem. B* **102**, 5914–5922 (1998).
- <sup>22</sup>J. D. Watson and F. H. C. Crick, *Nature* **171**, 737–738 (1953).
- <sup>23</sup>W. I. Sundquist and A. Klug, *Nature* **342**, 825–829 (1989).
- <sup>24</sup>K. Gehring, J.-L. Leroy, and M. Gueron, *Nature* **363**, 825–829 (1993).
- <sup>25</sup>M. Petersheim and D. H. Turner, *Biochemistry* **22**, 256–263 (1983).
- <sup>26</sup>E. T. Kool, *Annu. Rev. Biophys. Biomol. Struct.* **30**, 1–22 (2001).
- <sup>27</sup>C. A. Hunter and J. K. M. Sanders, *J. Am. Chem. Soc.* **112**, 5525–5534 (1990).
- <sup>28</sup>D. J. Frankel, Q. Chen, and N. V. Richardson, *J. Chem. Phys.* **124**, 204704 (2006).
- <sup>29</sup>M. Furukawa, H. Tanaka, and T. Kawai, *J. Chem. Phys.* **115**, 3419–3423 (2001).
- <sup>30</sup>M. Furukawa, T. Yamada, S. Katano, M. Kawai, H. Ogasawara, and A. Nilsson, *Surf. Sci.* **601**, 5433–5440 (2007).
- <sup>31</sup>W.-H. Li, W. Haiss, S. Floate, and R. J. Nichols, *Langmuir* **15**, 4875–4883 (1999).
- <sup>32</sup>T. Nakagawa, H. Tanaka, and T. Kawai, *Surf. Sci.* **370**, L144–L148 (1997).
- <sup>33</sup>R. Otero, M. Schöck, L. M. Molina, E. Lægsgaard, I. Stensgaard, B. Hammer, and F. Besenbacher, *Angew. Chem., Int. Ed.* **44**, 2270–2275 (2005).
- <sup>34</sup>S. Rapino and F. Zerbetto, *Langmuir* **21**, 2512–2518 (2005).
- <sup>35</sup>M. L. M. Rocco, R. Dudde, K. H. Frank, and E. E. Koch, *Chem. Phys. Lett.* **160**, 366–370 (1989).
- <sup>36</sup>H. Tanaka, T. Nakagawa, and T. Kawai, *Surf. Sci.* **364**, L575–L579 (1996).
- <sup>37</sup>W. Xu, R. E. A. Kelly, R. Otero, M. Schöck, E. Lægsgaard, I. Stensgaard, L. N. Kantorovich, and F. Besenbacher, *Small* **3**, 2011–2014 (2007).
- <sup>38</sup>T. Yamada, K. Shirasaki, A. Takano, and M. Kawai, *Surf. Sci.* **561**, 233–247 (2004).
- <sup>39</sup>Q. Chen, D. J. Frankel, and N. V. Richardson, *Langmuir* **18**, 3219–3225 (2002).
- <sup>40</sup>E. Rauls, S. Blankenburg, and W. G. Schmidt, *Surf. Sci.* **602**, 2170–2174 (2008).
- <sup>41</sup>F. Allegretti, M. Polcik, and D. P. Woodruff, *Surf. Sci.* **601**, 3611–3622 (2007).
- <sup>42</sup>M. Furukawa, H. Fujisawa, S. Katano, H. Ogasawara, Y. Kim, T. Komeda, A. Nilsson, and M. Kawai, *Surf. Sci.* **532–535**, 261–266 (2003).
- <sup>43</sup>D. C. Jackson, D. A. Duncan, W. Unterberger, T. J. Lerotholi, D. K. Lorenzo, M. K. Bradley, and D. P. Woodruff, *J. Phys. Chem. C* **114**, 15454–15463 (2010).
- <sup>44</sup>F. Kalkan, M. Mehlhorn, and K. Morgenstern, *J. Phys.: Condens. Matter* **24**, 394010 (2012).
- <sup>45</sup>S. Kilina, S. Tretiak, D. A. Yarotski, J.-X. Zhu, N. Modine, A. Taylor, and A. V. Balatsky, *J. Phys. Chem. C* **111**, 14541–14551 (2007).
- <sup>46</sup>A. McNutt, S. Haq, and R. Raval, *Surf. Sci.* **502**, 185–192 (2002).
- <sup>47</sup>A. McNutt, S. Haq, and R. Raval, *Surf. Sci.* **531**, 131–144 (2003).
- <sup>48</sup>R. Otero, M. Lukas, R. E. A. Kelly, W. Xu, E. Lægsgaard, I. Stensgaard, L. N. Kantorovich, and F. Besenbacher, *Science* **319**, 312–315 (2008).
- <sup>49</sup>O. Plekan, V. Feyer, S. Ptasińska, N. Tsud, V. Cháb, V. Matolín, and K. C. Prince, *J. Phys. Chem. C* **114**, 15036–15041 (2010).
- <sup>50</sup>I. Horcas, R. Fernández, J. M. Gómez-Rodríguez, J. Colchero, J. Gómez-Herrero, and A. M. Baro, *Rev. Sci. Instrum.* **78**, 013705 (2007).
- <sup>51</sup>G. Kresse and J. Furthmüller, *Phys. Rev. B* **54**, 11169–11186 (1996).
- <sup>52</sup>G. Kresse and J. Hafner, *Phys. Rev. B* **47**, 558–561 (1993).
- <sup>53</sup>S. Grimme, *J. Comput. Chem.* **27**, 1787–1799 (2006).
- <sup>54</sup>L. González and C. Daniel, *J. Comput. Chem.* **27**, 1781–1786 (2006).
- <sup>55</sup>J. Tersoff and D. R. Hamann, *Phys. Rev. Lett.* **50**, 1998–2001 (1983).
- <sup>56</sup>N. Lorente and M. Persson, *Faraday Discuss.* **117**, 277–290 (2000).
- <sup>57</sup>M. J. Frisch, G. W. Trucks, H. B. Schlegel, G. E. Scuseria, M. A. Robb, J. R. Cheeseman, G. Scalmani, V. Barone *et al.*, Gaussian 09, Gaussian, Inc., Wallingford CT, 2009.
- <sup>58</sup>M. P. Andersson and P. Uvdal, *J. Phys. Chem. A* **109**, 2937–2941 (2005).
- <sup>59</sup>M. D. Topal and J. R. Fresco, *Nature* **263**, 285–289 (1976).
- <sup>60</sup>D. B. Hall, R. E. Holmlin, and J. K. Barton, *Nature* **382**, 731–735 (1996).
- <sup>61</sup>P. Colarusso, K. Zhang, B. Guo, and P. F. Bernath, *Chem. Phys. Lett.* **269**, 39–48 (1997).
- <sup>62</sup>S. L. Zhang, K. H. Michaelian, and G. R. Lopnow, *J. Phys. Chem. A* **102**, 461–470 (1998).
- <sup>63</sup>K. L. Wierchowski, E. Litonska, and D. Shugar, *J. Am. Chem. Soc.* **87**, 4621–4629 (1965).
- <sup>64</sup>B. Lippert and D. Neugebauer, *Inorg. Chim. Acta* **46**, 171–179 (1980).
- <sup>65</sup>T. Giebel, O. Schaff, R. Lindsay, P. Baumgärtel, M. Polcik, A. M. Bradshaw, A. Koebbel, T. McCabe *et al.*, *J. Chem. Phys.* **110**, 9666–9672 (1999).
- <sup>66</sup>R. Terborg, M. Polcik, J. T. Hoeft, M. Kittel, M. Pascal, J. H. Kang, C. L. A. Lamont, A. M. Bradshaw, and D. P. Woodruff, *Surf. Sci.* **457**, 1–10 (2000).
- <sup>67</sup>X. Ye, Z.-H. Li, W. Wang, K. Fan, W. Xu, and Z. Hua, *Chem. Phys. Lett.* **397**, 56–61 (2004).
- <sup>68</sup>D. Leckband and J. Israelachvili, *Q. Rev. Biophys.* **34**, 105–267 (2001).